Available online at www.sciencedirect.com
SCIENCE DIRECT®
International Journal of Multiphase Flow 30 (2004) 1071–1091
International Journal of Multiphase Flow
www.elsevier.com/locate/ijmulflow

Investigation of thermocapillary convective patterns and their role in the enhancement of evaporation from pores

Cosimo Buffone, Khellil Sefiane *

School of Engineering and Electronics, The University of Edinburgh, Kings Buildings, Mayfield Road, Edinburgh EH9 3JL, Scotland, UK

Received 24 July 2003; received in revised form 20 May 2004

Abstract

The present work investigates the evaporation process from a liquid meniscus formed in capillary tubes of various sizes. A very strong convection within the liquid phase is observed; it is proposed that the non-uniform evaporation from the meniscus leads to a temperature gradient along the interface causing a surface tension gradient, which is the driving mechanism for the convection. The observed convection is shown to be clearly correlated to the evaporation rate and the volatility of the liquid. Unlike Marangoni convection observed by imposing a temperature gradient, this is a self-induced driving gradient caused by evaporative cooling effect.

The Marangoni roll in the liquid phase has been visualized and characterized using seeding particles. It is shown in the present study that the observed convection contribute in enhancing the heat–mass transfer from the pore. The experimental results show that when the meniscus recedes inside the pore, the convection slows down and eventually stops. A theoretical model is developed to describe the temperature gradient, which establishes due to the evaporative cooling effect between the centre and the wedge of the meniscus. The results of the model show a good qualitative agreement with the experimental observations.

Keywords: Microsystems; Confinement; Evaporation; Heat transfer; Convection; Diffusion; Thermocapillary; PIV

1. Introduction

In recent years, there has been an increasing interest for the phenomena involved in the evaporation of thin films because of potential applications in many two phase heat transfer

* Corresponding author. Tel.: +44-0131-650-4873; fax: +44-0131-650-6551.
E-mail address: ksefiane@chemeng.ed.ac.uk (K. Sefiane).

0301-9322/$ - see front matter
doi:10.1016/j.ijmultiphaseflow.2004.05.010

devices involving phase change. Although a lot of works have been done in the area (Chu, 1986; Mirzamoghadam and Catton, 1988; Swanson and Herdt, 1992; Pratt and Hallinan, 1997; Hallinan et al., 1998; Lee et al., 1999; Wei and Ma, 2002a,b; Wei et al., 2002), many open questions remain to be addressed because of the difficulties encountered in resolving and quantifying the micro-flows involved. Exploring this area and understanding the basic mechanisms involved is a key to improve the heat transfer capability of devices involving phase change in confined environments. In an early work Potash and Wayner (1972) investigated the transport processes that occurred in a two-dimensional evaporating meniscus and adsorbed thin film on a superheated flat glass plate immersed in a liquid. It was assumed that the local heat flux across the meniscus is fixed by the thermal resistance of the liquid. The work was able to conclude that a change in the profile of the meniscus brings about a pressure drop that is sufficient to circulate the fluid replacing the liquid that has evaporated and hence allows the evaporation to continue. It was also shown that in the intrinsic meniscus region fluid flow is brought about by thermocapillarity while in the evaporating thin film region the fluid flow is entirely caused by the disjoining pressure gradient between the film and the vapour. This is the force resulting from the pull of the adhesion forces between the adsorbed liquid molecules in the thin liquid film and the tube wall, i.e. liquid–solid interfacial forces, and it leads to the motion of liquid in the thin liquid film region. This result is backed up by previous research by Potash and Wayner which showed that, depending on the magnitudes of the heat and mass transfer coefficients, thermocapillary flows are unimportant in the upper region of the meniscus. Cook et al. (1981) were concerned with the heat transfer characteristics of the contact line region of an evaporating extended meniscus, given its large and efficient heat sink capabilities which could be made use of in industrial applications. Wayner and Tung (1985) studied how the bulk composition of a liquid mixture affects stationary, steady-state evaporating thin films. It was found that even small changes in the bulk composition could lead to significant changes in heat and mass transfer in the contact line region, and hence that the profile of the contact line is a strong function of both the evaporation rate and composition. It was also noted, however, that gradients in either temperature or concentration can lead to shear stresses at the interfaces and recirculation flows in the liquid which improve the stability of the meniscus in the contact line region. Khrustalev and Faghri (1994, 1996) investigated thermocapillary convection using grooved plates heated on the bottom. They set about establishing the influence of the liquid and vapour flows resulting from this effect on heat transfer from the meniscus formed by the liquid in the groove. They found that the convection currents formed in the liquid just below the meniscus could increase the heat transfer coefficient by up to 30%. This is presumably due to the assistance that the convection currents give in bringing liquid from the bulk region right up to the interface where the heat transfer occurs, and then removing it again. They also found that if there are very large temperature differences between the wall and the vapour saturation temperature, then recirculation of the vapour could appear above the meniscus in the region where the meniscus meets the container wall. This is a very important factor in the design of micro-heat pipes because of the effects it will have on heat transfer capacity from the meniscus.

Szymczyk (1991) and Molenkamp (1998) showed that in containers with diameter greater than a few millimeters, Rayleigh convection or buoyancy dominates the convection process. Marangoni and Rayleigh convections are always coupled when a temperature difference exists inside a media with a free surface in g-environment. However, Rayleigh convection plays a more

important role when the flow characteristic dimension is large; instead, Marangoni convection is predominant at smaller scales.

The evaporation of a liquid meniscus formed in a capillary tube is the case investigated in the present paper. The liquid evaporates essentially in the thin film region of the meniscus in contact with the tube wall and we tried to quantify the phenomena involved. The focus of the present work is to investigate the evaporation in small capillary tubes with internal diameter ranging from 200 to 900 μm of volatile liquids (ethanol, methanol, acetone and *n*-pentane). The meniscus region in the liquid phase has been the object of the study. The convection roll has been characterized using tracers and the spinning frequency was measured. The evaporation rate was monitored following the receding meniscus. The objective is to correlate the evaporation process to the observed convection and to demonstrate how the latter contribute to the heat–mass transfer enhancement from the pore.

2. Experimental apparatus and procedure

The borosilicate glass capillaries used in the present investigation were bought from Drummund Scientific. These were cleaned using an ultrasonic bath with de-ionized water for 30 min at 65 °C and dried in an oven at 60 °C for 2 h. The tubes were stored in a clean vial and used within few days. To avoid contamination, capillaries were filled from the end opposite to that where the meniscus was positioned for observation.

The roughness of the internal tube surface was characterized using a profilometer (manufactured by Zygo Corporation). The use of the profilometer allowed us to analyze surfaces with a high curvature. Large pieces have been cut and the analysis was performed far away from the edges to avoid edge effects. Two important parameters are used to characterize the surface roughness, R_a and rms (Farshad et al., 2001). The R_a is defined as the average surface roughness. The rms is defined as the root mean square average of the measured height deviation. The surface roughness parameters are reported in Table 1. In order to compare the roughness of the present case, it is more appropriate to normalize both R_a and rms with the pore diameter, following Li et al. (2002), rather than with a surface length. From the analysis of the relative surface roughness (defined as the ratio of R_a to internal tube radius) reproduced in Table 1, the tubes can be considered as smooth.

All liquids used were bought from Sigma-Aldrich; their physical properties are given in Table 2 from Yaws (1999). The experimental set-up sketched in Fig. 1 comprises an Olympus Research microscope with an attached high-speed camera (Phantom v4.3) capable of 1000 frames per second at 512×512 pixels. An acquisition computer is used to acquire sequences from the camera,

Table 1
Tube surface roughness analysis (samples dimensions 140×110 μm)

ID (μm)	R_a (nm)	Rms (nm)	Relative roughness (%) $\times 10^{-4}$
200	1.354	1.741	6.77
600	3.479	4.588	5.79
900	4.105	5.094	4.56

Table 2
Liquids properties at 1 atm and 25 °C (from Yaws (1999))

Liquids	Boiling point (°C)	P_v (N m^{-2}) $\times 10^3$	ΔH (kJ mol^{-1})	c_{pl} (J/mol K) $\times 10^2$	ρ_l (kg/m^3) $\times 10^2$	k_l (W/m K) $\times 10^{-1}$	μ_l (N s/m^2) $\times 10^{-8}$	σ (dynes/cm)
Ethanol	78.4	7.61	40.3	0.798	7.88	2.01	5.45	23.6
Methanol	64.7	16.2	38.0	1.073	7.88	1.69	10.7	23.5
Acetone	56.5	29.8	32.2	1.274	7.86	1.62	3.09	23.1
n-Pentane	36.3	66.8	26.7	1.635	6.22	1.48	2.46	15.5

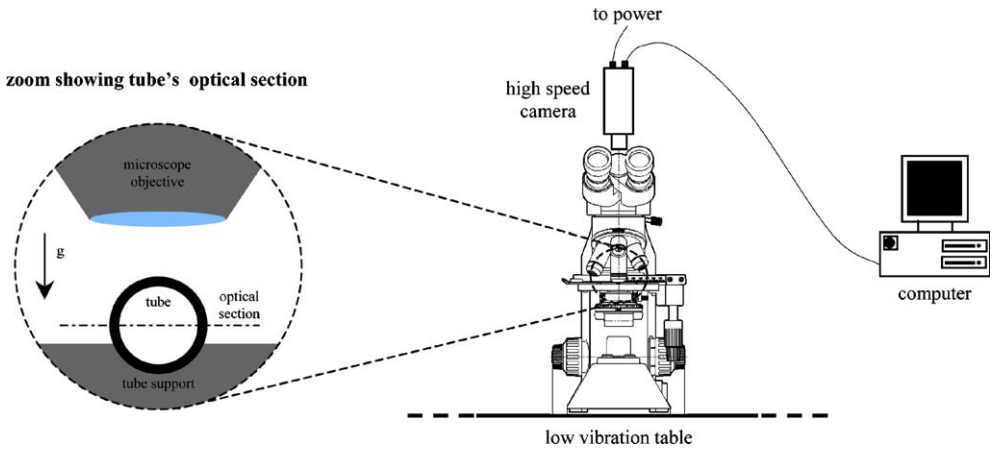

Fig. 1. Schematic of the experimental set-up.

which are analyzed using specialized software. An IR filter has been placed between the light and the condenser of the microscope to avoid transfer of heat via light into the capillary. Preliminary tests showed how the meniscus oscillates when receding inside the pore and the evaporation rate is higher without the filter. All the experiments have been performed with the tubes in horizontal position and making horizontal optical section with the microscope on an optical low vibration table. Particles have been used as tracers in the liquid phase to visualize and characterize convection motion (see Fig. 2a). The tracers were nylon spherical particles with mean diameter of 20 μm. For PIV measurements, borosilicate glass particles (spherical particles from Potters Industrial Inc.) with 7–26 μm diameter (depending on the capillary size) were used. Fig. 2b shows an example of PIV analysis results where two counter-rotating vortices are observed. For the PIV plot, the velocity vector map, streamline and superimposed vorticity map are reproduced in each image.

Two types of experiments have been performed. In Experiment (1) (see sketch in Fig. 3), the meniscus has been positioned at the capillary mouth using a micro-syringe, then was left free to move inside the pore. When the capillary was filled with the volatile liquids, particular care has been taken to avoid the formation of bubbles along the system syringe/polyamide tube/capillary. In fact, it has been noticed that the presence of bubbles strongly influences the results. Each capillary was used only once. In Experiment (2) (see Fig. 3) both ends of the capillary were open

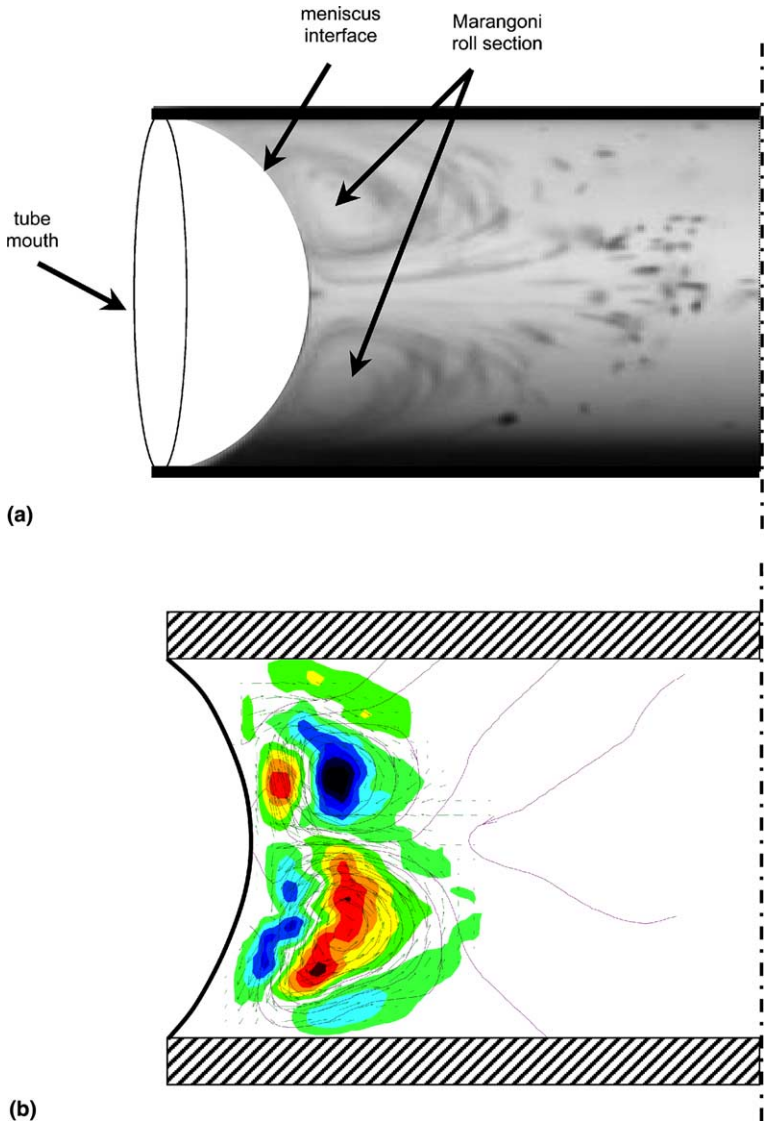

Fig. 2. Visualization of the liquid flow pattern using seeding tracers: (a) optical section of the capillary tube; (b) PIV analysis with superimposed vector map, streamlines and vorticity map.

allowing the formation of two menisci: one meniscus was stuck at the capillary mouth (where convection motion was monitored) while the other recedes inside the pore (used to evaluate the evaporation rate) as evaporation takes place.

In both experiments the evaporation is self-sustained because of the liquid volatility. The necessary heating for this process comes from the capillary tube's surrounding environment and no extra heating is provided by any means. In fact, the liquid evaporating cools down the meniscus interface bringing its temperature below the room one setting about an heat transfer mechanism through the conductive tube's wall.

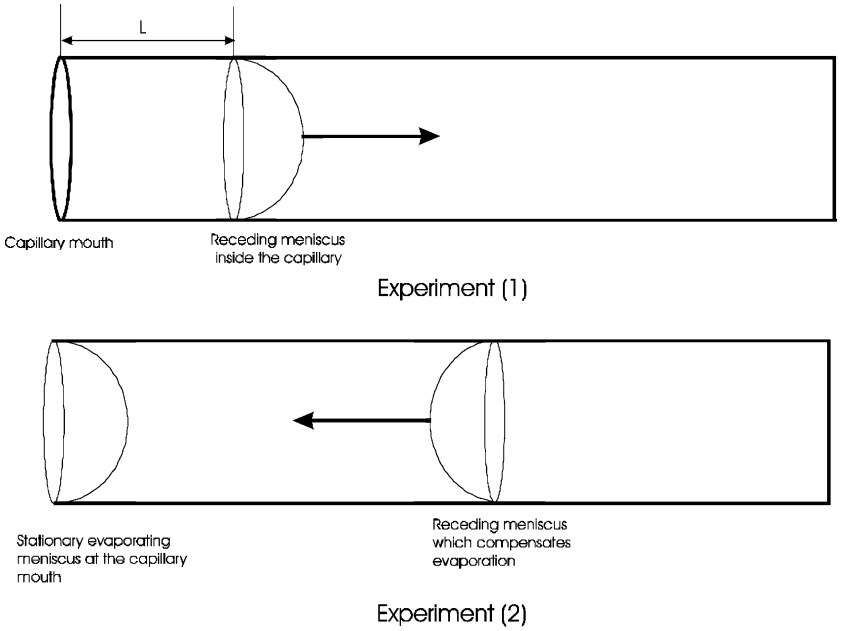

Fig. 3. Experimental sketch: Experiment (1) with one receding meniscus; Experiment (2) with two menisci.

During each experiment, the environmental conditions (temperature, relative humidity) were monitored. The room temperature and relative humidity were of 25 ± 2 °C and $50 \pm 5\%$ respectively. Preliminary tests made at different times showed that the environmental conditions play a marginal role; the largest difference found on the evaporation rate was 3–4%. A motion analysis software (MAStudio) for tracking and analysis was used. For PIV analysis a specialized software (FlowMap from Dantec Dynamics) was used.

3. Results

In Experiment (1) (see Fig. 3) the meniscus moves inside the pore as evaporation takes place. The meniscus moves in two distinct stages; first, it changes shape but remains stuck at the capillary mouth due to the strong adhesion forces. When the receding apparent contact angle is reached, it starts to recede inside the pore. As the meniscus recedes evaporation continues however, vapour has to diffuse to the mouth of the capillary. As a result, the partial vapour pressure at the liquid–vapour interface builds up as the meniscus recedes inside the pore. The difference between the vapour partial pressure and its saturation value is the driving force for evaporation.

The distance of the meniscus measured from the tube mouth (L) is reported in Fig. 4 as a function of time for *n*-pentane and various capillary sizes. This would allow us to evaluate the evaporation rate. In order to emphasize the difference between different volatile liquids, Fig. 5 shows the meniscus position vs. time for 600 μm pore size for various liquids. From Figs. 4 and 5 it is clear that the slope of the curves (corresponding to the evaporation rate) increases noticeably

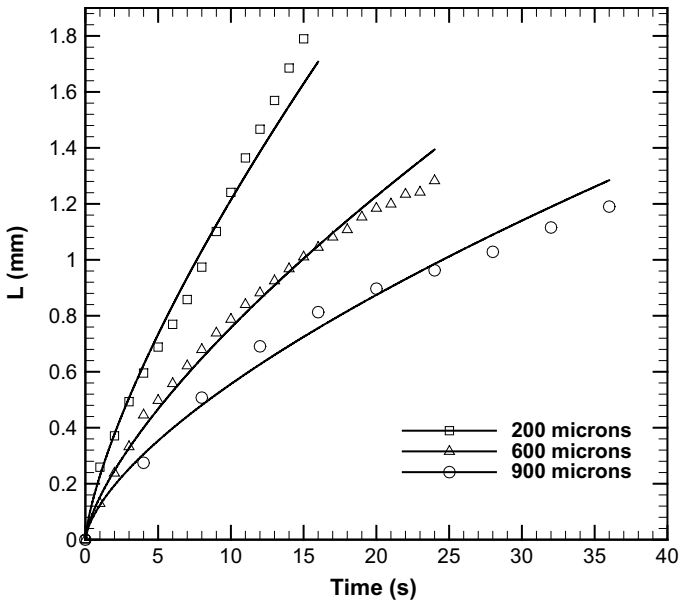

Fig. 4. Experiment (1): meniscus position from the tube mouth (L) for n-pentane and various tube sizes (experimental points and best fit).

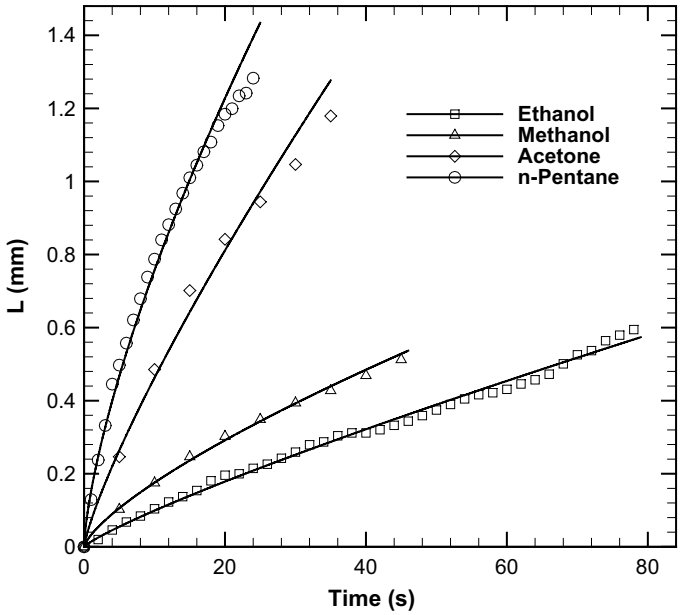

Fig. 5. Experiment (1): meniscus position from the tube mouth (L) for 600 μm and four different liquids (experimental points and best fit).

with smaller tube size and with the use of more volatile liquids. The slope of each curve decreases also as the meniscus recedes inside the tube for the reason pointed out earlier about the partial vapour pressure rise.

In Experiment (1) the liquid adjacent to the interface was seeded with particles as tracers to reveal the flow pattern. The frequency of the convection roll has been measured as the meniscus recedes inside the capillary. Fig. 6 shows the tracers' spinning frequency for ethanol and methanol and various tube sizes vs. the meniscus position (L) from the tube mouth. The tracers' spinning frequency increases as the tube size decreases for both liquids and decreases dramatically as the meniscus recedes inside the capillary; the frequency also increases with the liquid volatility. For the case of ethanol in 900 μm tube, the PIV analysis was performed and shown in Fig. 7. Note that a reference vector is plotted at the top left corner of each PIV image. As the meniscus moves deeper inside the pore the strength of the convection (indicated by the vorticity) is weakened.

The results for the evaporation rate and spinning frequency demonstrate the strong link between the evaporation process and the observed convection. The rolls shape and dimensions and their evolution have also been monitored. As the meniscus starts to move changing first its shape, the rolls are stretched in the direction of the movement. When the meniscus detaches starting to recede, the roll shape and dimensions do not further change noticeably. Therefore it can be stated that the roll shape and dimensions vary in accordance with the change of the meniscus profile. As the meniscus detaches from the capillary mouth, its profile remains unchanged although the driving force for evaporation changes because of the vapour pressure rise; this do not appreciably influences the roll shape and dimensions, but only its spinning frequency.

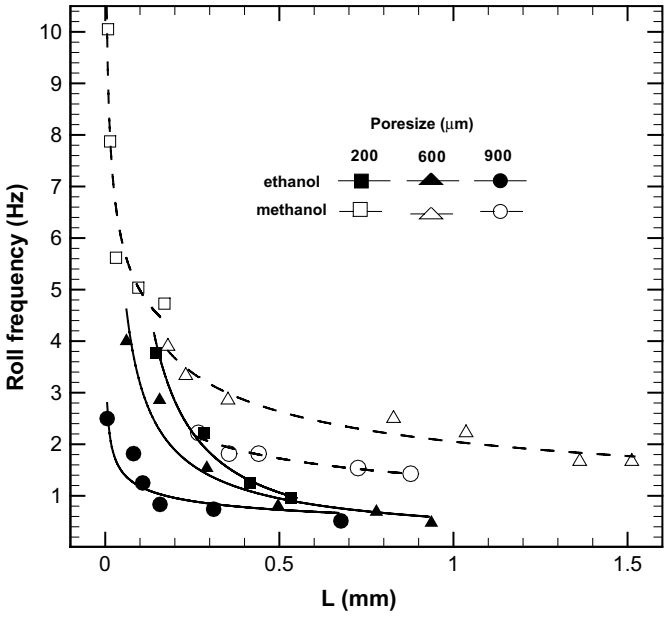

Fig. 6. Experiment (1): tracer spinning frequency comparison for ethanol and methanol and three tube sizes (experimental points and best fit).

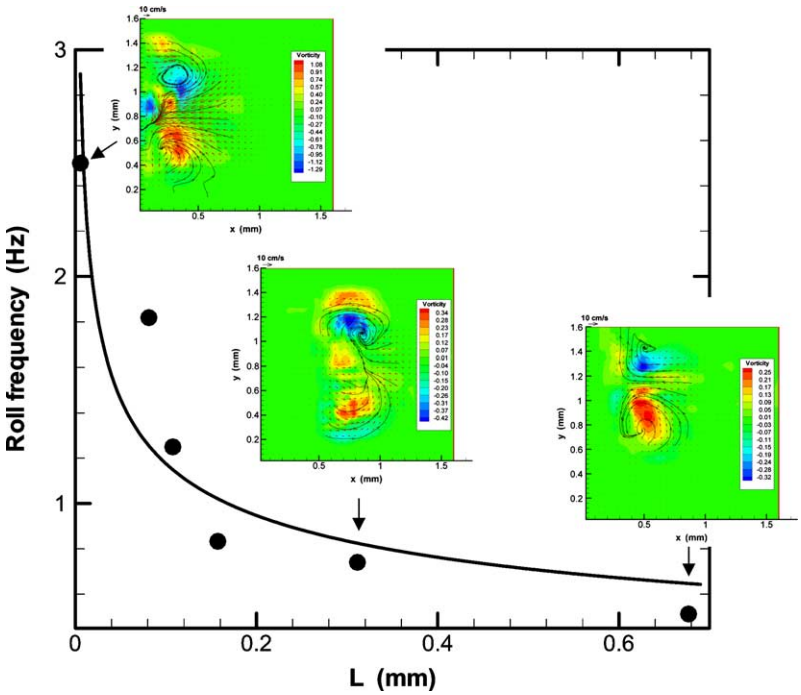

Fig. 7. Experiment (1): roll frequency and PIV analysis for the case of ethanol and 900 μm tube size.

The second Experiment (2) consists of partially filling a tube and leave both ends open. In this case two menisci are formed along the pore (see Fig. 3). The evaporation takes place at both menisci inside the capillary tube; one meniscus remains stuck at the pore mouth due to the stronger adhesion forces while the other recedes inside the capillary. However, the evaporation at the receding meniscus is of less importance; in fact, Experiment (1) demonstrated how the evaporation dramatically weakens as the meniscus moves far from the pore mouth. Following the receding meniscus along the pore, experiments conducted on each tube size and for each liquid confirm the assumption that evaporation from the receding meniscus is negligible. The evaporation rate measured changes of less than 5–7% over a length of 5–25 times the internal tube diameter (depending upon the tube size); then, the difference is reduced with smaller tube size and with the use of more volatile liquid. Therefore the velocity of the receding meniscus is exactly the rate of evaporation taking place in the meniscus stuck at the capillary mouth. The liquid on the meniscus stuck at the capillary mouth was seeded with particles to characterize convection. The evaporation rate and the spinning frequency of convection rolls have been correlated. In order to compare the average evaporation flux, the results on evaporation rate have been referred to the spherical cap area rather than to the tube cross-section area. The assumption of considering the meniscus as a spherical cap is a good approximation when gravity can be neglected as shown by Kim (1994). Fig. 8 shows both the evaporation rate and its averaged flux for different liquids and tube sizes. The overall evaporation rate increases for all liquids with increasing the tube size and with the use of a more volatile liquid; this is essentially due to a larger available surface area for evaporation for bigger tube size. On the contrary, the average evaporation flux decreases with

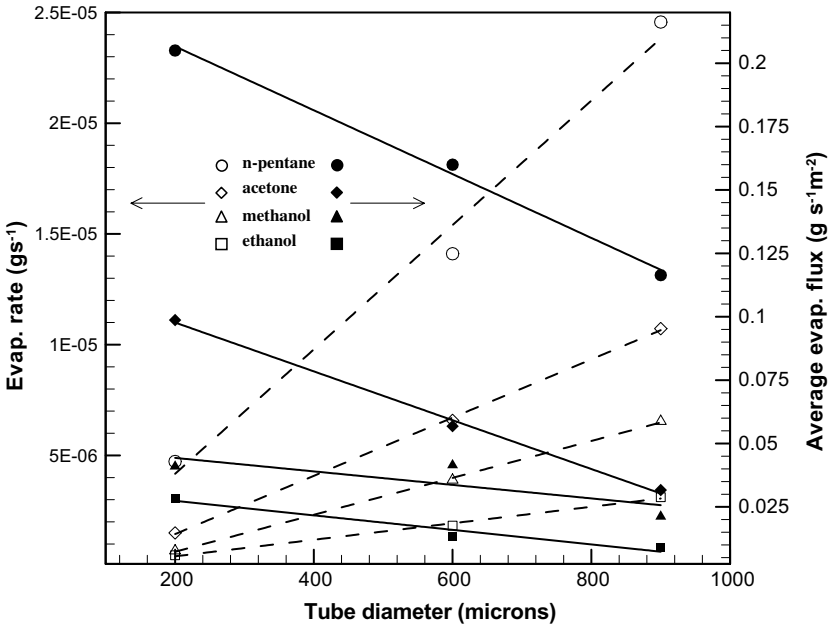

Fig. 8. Experiment (2): evaporation rate and average evaporation flux vs. tube size.

increasing the tube size. In order to point out the strong link between the evaporation process and the observed convection, the average evaporation flux and the tracers' spinning frequency have been correlated in Fig. 9 for the case of ethanol; both of these parameters are found to increase when the tube size decreases. Note that in Fig. 9 for completeness the evaporation heat flux is also reported. PIV analysis is presented and looking at the magnitude of vorticity confirms the stronger convection at smaller tubes sizes. Note that for 200 μm size, only the upper roll section is shown.

4. Theoretical model

The thermocapillary motion observed in our experiments is due to a thermal gradient established along the meniscus interface, which takes its origin in the strong evaporation occurring at the triple line region while the centre of the spherical cap undergoes a weaker evaporation. Evaporation takes place at the interface then vapour diffuses to the mouth of the capillary. In the following, we will attempt to calculate the temperature at the triple line region by a heat diffusion model. The temperature at the apex of the spherical cap, where evaporation is much less intense than in the wedge, is assumed equal to the temperature of the bulk liquid; this last is taken equal to the ambient temperature (see Fig. 10).

A sketch of the heat transfer paths for the present case is shown in Fig. 11. Evaporation takes place along the meniscus interface producing a local drop in temperature. A heat transfer mechanism is set in and heat is transferred from the environment outside the tube to the meniscus

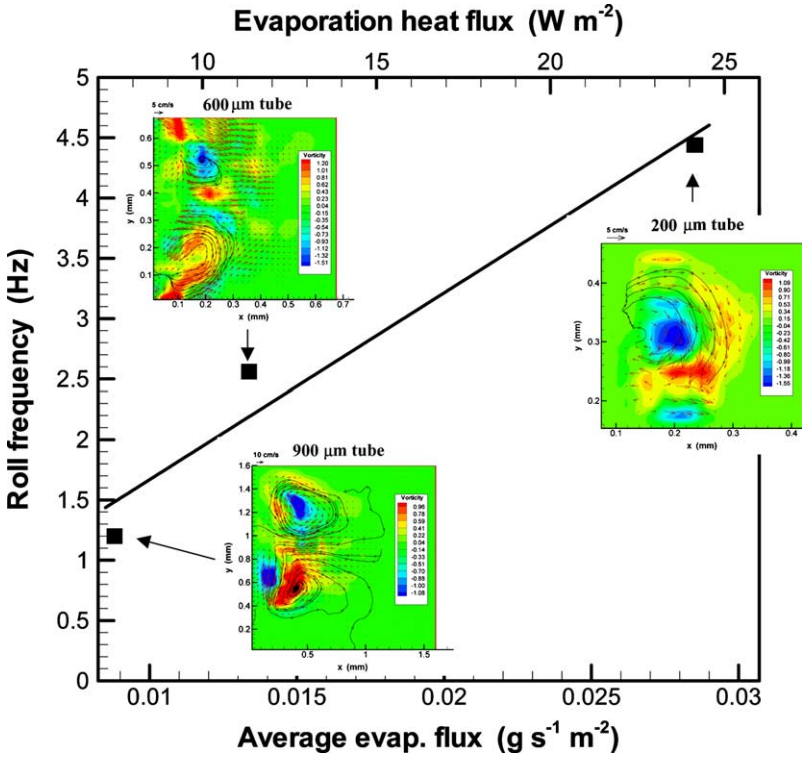

Fig. 9. Experiment (2): tracer spinning frequency vs. evaporation flux with PIV analysis for ethanol and various tube sizes.

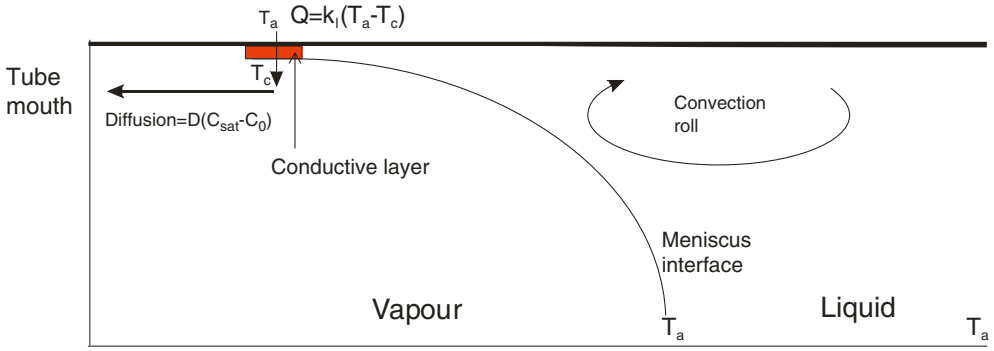

Fig. 10. Conduction–diffusion model from a receding meniscus.

interface, passing through the tube walls and the thin liquid layer. For an order of magnitude analysis, it is reasonable to neglect the heat conducted along the tube walls (Q_{wallCond}). The vapour can be assumed to be ''passive'' (see Meyer, 1984; Shieh, 1985; Davis, 1987; Riley, 1996; Pratt, 1996) because it has negligible viscosity, density and thermal conductivity compared to the liquid. The shear stresses at the interface due to surface tension gradients produce in the liquid phase the

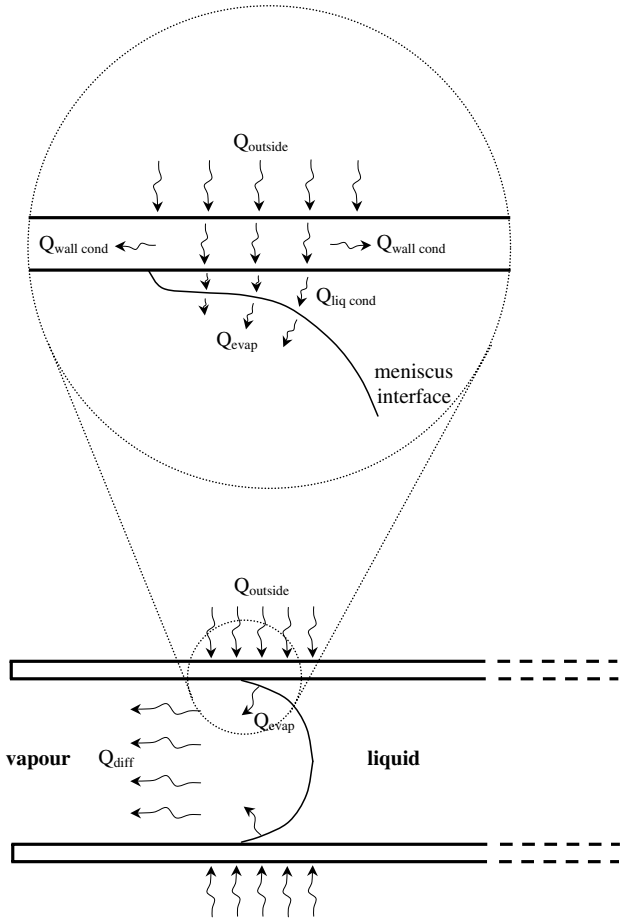

Fig. 11. Heat paths sketch for an evaporating-receding meniscus.

motion observed in this study by dragging the viscous liquid along the interface from hot to cold regions. Because of the very low vapour viscosity, the same stresses do not produce vapour recirculation. Therefore, in accordance with other authors (Meyer, 1984; Shieh, 1985; Davis, 1987; Riley, 1996; Pratt, 1996) we can assume here that the mass transfer mechanism in the vapour phase is dominated by diffusion. It is worth mentioning that a method namely the WIKELMANN technique (Coulson and Richardson, 1999) adopting an experimental set up similar to the one analyzed here, is widely used to determine the diffusion coefficient. In the WIKELMANN method, a liquid is allowed to evaporate in a vertical glass tube closed at the bottom and open at the top, and the rate of evaporation can be measured by following the falling meniscus. It is advisable to use capillary tubes smaller than 500 μm (same order or magnitude as in the present case) to ensure that the mass transfer to the tube top mouth takes place by molecular diffusion alone (Berezhnoi and Semenov, 1997). Therefore, we can reasonably assume that what evaporates from the meniscus interface is diffused in the gas phase ($Q_{\text{evap}} = Q_{\text{diff}}$). In other words, the mass flux at the wedge surface in the steady state is equal to the diffusion mass flux in the vapour.

The diffusion mass flux ($\dot{m}$) can be expressed as

$$\dot{m} = MD\nabla C = MD\frac{\partial C}{\partial L} \tag{1}$$

where M is the vapour molecular weight, D is the diffusion coefficient, C is the vapour concentration into air and L is the meniscus distance from the tube mouth. Eq. (1) becomes

$$\dot{m} = \frac{M}{L}DC_{\text{sat}} \tag{2}$$

where the surface vapour concentration of the volatile liquid in air at the wedge corner is assumed to be the saturation one (C_{sat}) and the concentration at the mouth of the capillary is assumed to be very small ($=0$).

As will be discussed in the next section, along the meniscus interface most of the evaporation takes place in the meniscus micro-layer region (see Fig. 10). This layer is of paramount importance in the heat and mass transfer from a meniscus interface as shown by different authors (Dejaguin, 1965; Moosman and Homsy, 1980; Schonberg et al., 1995; Park and Lee, 2003); this layer has a thickness of the order of $h = 5$–15 μm and is extended for $l_{\text{evap}} = 17.5$ μm (see Park and Lee, 2003). Because of its small thickness no convection can set in and the layer is commonly assumed purely conductive (see Moosman and Homsy, 1980).

The local energy balance ($Q_{\text{evap}} = Q_{\text{liq cond}}$) at the surface of the conducting layer region of the meniscus reads

$$\dot{m}\frac{\Delta H}{M}A_{\text{diff}} = \kappa_{\text{l}}\vec{\nabla}T_{\text{l}} \cdot \vec{1}A_{\text{evap}} \tag{3}$$

where ΔH is the latent heat of evaporation, κ_{l} is liquid thermal conductivity, $\vec{\nabla}T_{\text{l}}$ is the temperature gradient, $\vec{1}$ is the unity vector, the $A_{\text{evap}} = 2\pi R_{\text{i}} l_{\text{evap}}$ and $A_{\text{diff}} = \pi R_{\text{i}}^2$. Eq. (3) states that all what evaporates at the meniscus wedge has to diffuse through the cross-section of the tube.

We then write for the normal component of the heat flux:

$$\dot{m}\frac{\Delta H}{M}A_{\text{diff}} = \kappa_{\text{l}}\frac{T_{\text{a}} - T_{\text{c}}}{h}A_{\text{evap}} \tag{4}$$

where h is the mean thickness of the conductive layer (assumed for calculation purposes in the model as $h = 10$ μm), T_{c} is the temperature at the meniscus wedge and T_{a} is the wall temperature, this last being assumed to be the ambient air temperature for a conducting wall. Combining Eqs. (2) and (4) we get

$$D\frac{C_{\text{sat}}}{L}\Delta H\frac{A_{\text{diff}}}{A_{\text{evap}}} = \kappa_{\text{l}}\frac{(T_{\text{a}} - T_{\text{c}})}{h} \tag{5}$$

The saturation concentration can be written as

$$C_{\text{sat}} = \frac{P}{\Re T_{\text{c}}}x(T_{\text{c}}) \tag{6}$$

where P is the total pressure in the gas phase, $\Re$ is the gas constant and x is the mole fraction.

Clausius–Clapeyron relation is used to find the mole fraction as function of temperature:

$$x(T_c) = \exp\left[-\frac{\Delta H}{\Re}\left(\frac{1}{T_c} - \frac{1}{T_b}\right)\right] \tag{7}$$

where T_b is the liquid boiling temperature. We can thus re-write Eq. (5) as follows:

$$D\frac{P}{\Re T_c}\frac{\Delta H}{L}\exp\left[-\frac{\Delta H}{\Re}\left(\frac{1}{T_c} - \frac{1}{T_b}\right)\right]\frac{A_{diff}}{A_{evap}} = \kappa_l\frac{(T_a - T_c)}{h} \tag{8}$$

Solving the above equation will give us the temperature of the interface at the meniscus wedge. This would allow us to estimate the variation of the temperature gradient $(T_a - T_c)$ as a function of the distance of the meniscus from the capillary mouth L.

If we define the dimensionless length $\widetilde{L} = \frac{h}{L}$, and substitute $\frac{A_{diff}}{A_{evap}} = \frac{R_i}{2l_{evap}}$ Eq. (8) is written as follows:

$$\frac{D\Delta HP}{\Re\kappa_l}\frac{R_i}{2l_{evap}}\widetilde{L}\exp\left[-\frac{\Delta H}{\Re}\left(\frac{1}{T_c} - \frac{1}{T_b}\right)\right] = T_c(T_a - T_c) \tag{9}$$

Table 3 shows the results giving the temperature difference $(T_a - T_c)$ between the wedge and the centre of the meniscus as the meniscus recedes inside the capillary ($\widetilde{L}$ diminishes). This indicates that the temperature difference between the apex and the wedge diminishes as the meniscus recedes inside the capillary. According to Table 3, the temperature difference $(T_a - T_c)$ is drastically reduced after $\widetilde{L} = 0.01$ (corresponding to $L = 1$ mm), therefore the driving force is weakened as the meniscus moves deeper inside the tube and the convection slows down; this is in agreement with the experimental results shown in Fig. 6.

The temperature that sets in at the corner T_c is lower than the temperature T_a at the centre of the cap and the Marangoni number (ratio between surface tension and viscous forces) is then defined as

Table 3
Temperature gradient and Marangoni number as a function of the dimensionless distance computed from the model ($T_a = 298$ K)

$\widetilde{L} = h/L$	Ethanol		Methanol	
	$T_a - T_c$ (K)	Ma	$T_a - T_c$ (K)	Ma
1	6.138	3308.32	10.235	9802.02
0.9	5.66	3050.68	9.527	9123.97
0.8	5.161	2781.72	8.776	8404.97
0.7	4.637	2499.29	7.974	7636.67
0.6	4.087	2202.85	7.115	6814
0.5	3.507	1890.24	6.19	5928.14
0.4	2.893	1559.3	5.187	4967.57
0.3	2.241	1207.88	4.091	3917.93
0.2	1.547	833.817	2.881	2759.12
0.1	0.802	432.27	1.531	1466.23
0.01	0.083	44.736	0.163	156.104
0.001	0.008	4.31192	0.016	15.3231

$$Ma = \frac{\partial\sigma}{\partial T}\nabla T_{\mathrm{l}}\frac{\rho_{\mathrm{l}}c_{p\mathrm{l}}}{\mu_{\mathrm{l}}\kappa_{\mathrm{l}}}d^2 = -\frac{\partial\sigma}{\partial T}(T_{\mathrm{a}} - T_{\mathrm{c}})\frac{\rho_{\mathrm{l}}c_{p\mathrm{l}}}{\mu_{\mathrm{l}}\kappa_{\mathrm{l}}}R_{\mathrm{i}}\frac{\left(\frac{\pi}{2} - \theta\right)}{\cos\theta} \tag{10}$$

where σ is the surface tension, ∇T_{l} the liquid temperature gradient along the meniscus interface, ρ_l, $c_{p\mathrm{l}}$, μ_{l} and k_{l} are the liquid density, specific heat capacity, dynamic viscosity and thermal conductivity respectively, and θ is the steady apparent contact angle. As characteristic dimension, the meniscus arc length d is taken:

$$d = R_{\mathrm{i}}\frac{\left(\frac{\pi}{2} - \theta\right)}{\cos\theta} \tag{11}$$

The temperature gradient is taken as

$$\nabla T_{\mathrm{l}} = \frac{(T_{\mathrm{a}} - T_{\mathrm{c}})}{R_{\mathrm{i}}\frac{\left(\frac{\pi}{2} - \theta\right)}{\cos\theta}} \tag{12}$$

One can describe the variation of the Marangoni number as a function of the distance of the meniscus from the mouth of the capillary tube, using the corresponding thermophysical properties of the appropriate liquid (Table 2). The profile of the Marangoni number versus the normalized length $\widetilde{L}$ can be obtained by solving Eq. (9) to find the temperature difference $(T_{\mathrm{a}} - T_{\mathrm{c}})$ and then use it to calculate the Marangoni number (also reported in Table 3). Results for a meniscus of ethanol and methanol receding in a 600 μm capillary tube are presented in Fig. 12 and show that Marangoni number decreases as the meniscus recedes inside the pore ($\widetilde{L}$ diminishes). Another important trend found is that methanol (more volatile) exhibits higher Marangoni numbers. Again, this qualitatively agrees with our findings reproduced in Fig. 6 in terms of tracer spinning frequency.

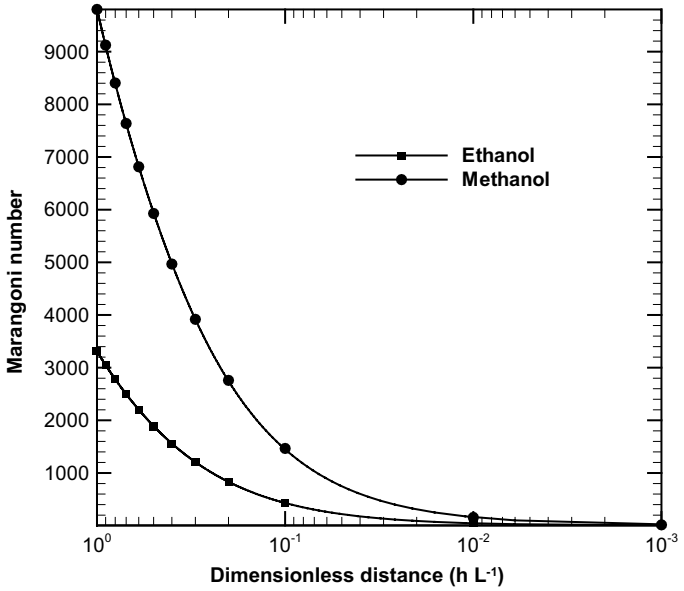

Fig. 12. Experiment (1): Marangoni number vs. dimensionless distance for two liquids and 600 μm tube.

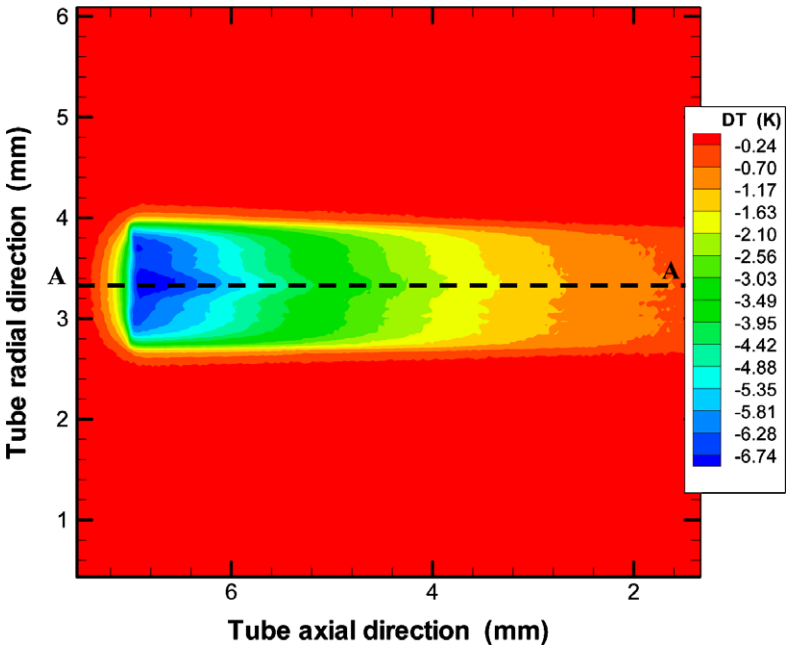

Fig. 13. IR measurement of 900 μm tube from the side and methanol as liquid (adapted from Buffone and Sefiane (in press)).

The temperature close to the meniscus triple line has been measured using an infrared camera for Experiment (2) and the procedure and results have been discussed in Buffone and Sefiane (in press). Fig. 13 reproduces the typical infrared measurement of the evaporating meniscus taken from the tube side and Fig. 14 shows the temperature profile extracted along the tube axis **A**–**A** (for clarity a sketch of the tube section is shown and the meniscus position location is indicated). Note that the temperature in Figs. 13 and 14 is the difference between the liquid and the ambient ones (the temperature deep gives $(T_a - T_c)$). In Fig. 14, the tube mouth is on the right side. The deep in temperature close to the tube mouth is the experimental evidence of the strong evaporation at the meniscus wedge. In Table 4, we show $(T_a - T_c)$ as measured by the infrared camera for methanol and ethanol and two tube sizes; note that no infrared measurement is available for 200 μm tube. It is clear that the temperature difference $(T_a - T_c)$ is larger for the more volatile liquid (methanol) and the smaller tube. There is a good qualitative agreement between these infrared measurements and the order of magnitude of the model presented in this section.

5. Discussion

The evaporation along the meniscus formed inside a confined space such as a pore is not uniform. It is larger near the wall than in the middle of the capillary (Sartre et al. (2000)). The results about the evaporation rate reproduced in Fig. 8 confirm this assumption. Indeed if the evaporation was uniform along the meniscus, we should have a linear relation between the

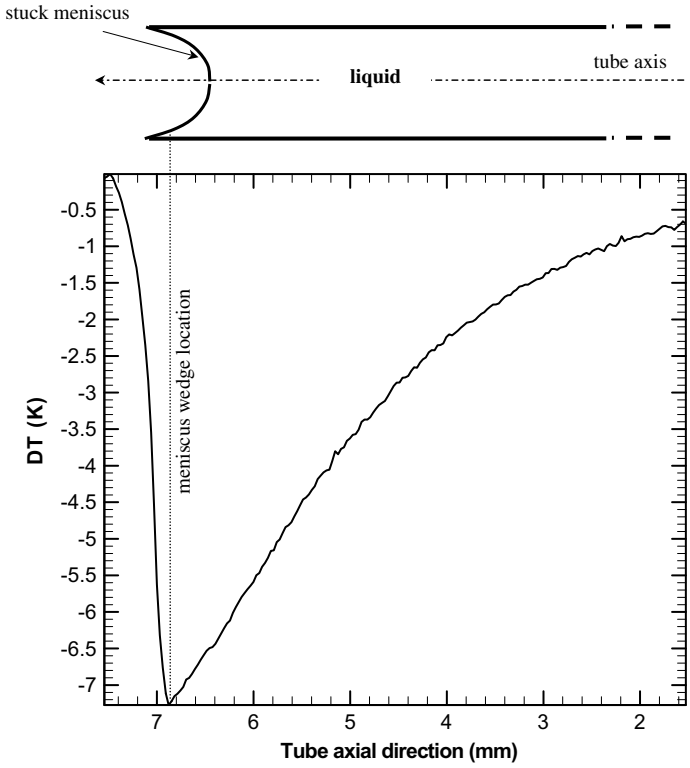

Fig. 14. Axial section (A–A) of the IR image in Fig. 12 (adapted from Buffone and Sefiane (in press)).

Table 4
Ambient temperature (T_a) menus temperature at the meniscus wedge (T_c) (InfraRed measurements taken from Buffone and Sefiane (in press))

Liquid	Tube size (μm)	$T_a - T_c$ (K)
Methanol	600	11.96
	900	7.20
Ethanol	600	8.09
	900	3.59

evaporation rate and the meniscus surface area, the latter being proportional to the square of the tube radius. The evaporation rate is linearly proportional to the tube radius and therefore is non-uniform along the meniscus, being stronger near the wall. The meniscus region close to the tube wall is usually (Potash and Wayner, 1972; Swanson and Herdt, 1992; Schonberg et al., 1995) divided in three different sub-regions. In the adsorbed layer of constant thickness the van der Walls forces dominate and no evaporation takes place. In a very tiny region (usually few percents of the entire meniscus length) most of the evaporation takes place because the adhesion forces are balanced by the capillary ones; this sub-region is called micro-region. As the meniscus thickness increases in the macro-region, the thermal resistance of the layer increases accordingly and the

heat transfer coefficient weaken as reported by Kim (1994). In the macro-region, the capillary forces dominate and set about a flow to re-supply the liquid evaporated in the micro-region. Bigger tube sizes have larger micro-region; in particular, the micro-region increases linearly with the tube radius. This is believed to be one of the possible reason of a linear increase in the evaporation rate with the tube radius shown in Fig. 8.

The non-uniform evaporation cools the liquid phase differentially along the meniscus interface leading to a difference in interfacial temperature and thus in surface tension and density along the meniscus interface. For small tubes (below 1 mm) the surface tension effect is predominant as pointed out by Szymczyk (1991) and Molenkamp (1998). Therefore, the surface tension gradient is expected to be the driving force for the thermal Marangoni convection roll visualized in the liquid phase (see Fig. 2). It is worth mentioning that similar conclusions have been reached, investigating the evaporation of sessile drops by Deegan et al. (2000). The analogy between the present case and a sessile drop is justified. The strong evaporation that is taking place near the triple line is governed by the same mechanism for both cases. Inside a pore, the convection roll has a toroidal shape and looking at it from the side with a microscope two sections can be seen (see Fig. 2). In the spinning movement, the particles are accelerated along the meniscus interface from the centre to the wedge; from there they move back along the walls to the bulk phase returning to the centre of the capillary and then are accelerated again along the capillary centre towards the meniscus. PIV technique has been used to characterize the so observed convection. The velocity field as well as the vorticity have been obtained. As mentioned in Section 3, the average evaporation flux is found to increase when reducing the tube size essentially because the evaporation rate increases linearly with the tube radius whereas the meniscus spherical cap area is proportional to the square of the tube radius. At the same time, the intensity of the convection rolls increases because of a higher temperature gradient along the meniscus interface. It is well established that convection helps the heat–mass transfer. Also for the present case, the role played by Marangoni convection is not negligible in bringing hot liquid from the bulk close to the meniscus interface where the heat–mass transfer is taking place because of evaporation.

Although convection contributes to the enhancement of the average evaporation flux, a time-scale analysis has shown that for the investigated system most of the energy (heat) necessary for sustaining evaporation comes through the walls of the capillary. Another important effect must be taken into account considering Experiment (1). The diffusion in the vapour phase plays also an important role. With the meniscus stuck at the capillary mouth, the evaporation is limited by the amount of heat brought from the surrounding environment. When the meniscus detaches from the pore mouth and starts to move inside the tube, the limiting mechanism for evaporation is the diffusion of vapour inside the pore. Results in Figs. 5 and 6, show that for various capillary sizes and liquids, evaporation is reduced when the meniscus recedes inside the pore. Measurements on convection (see Figs. 7 and 8), demonstrate that the spinning intensity decreases as well. The model developed earlier attempted to demonstrate how the temperature gradient along the meniscus interface responsible for the observed convection decreases as the meniscus recedes inside the pore.

In order to evaluate the role of the strong evaporation occurring at the meniscus micro-region, a comparison with an analytical model developed by Gamayunov and Lankov (1985) on a receding evaporating meniscus inside a pore has been performed. Gamayunov and Lankov (1985) model describes the evaporation rates in capillary tubes, without accounting for any convection

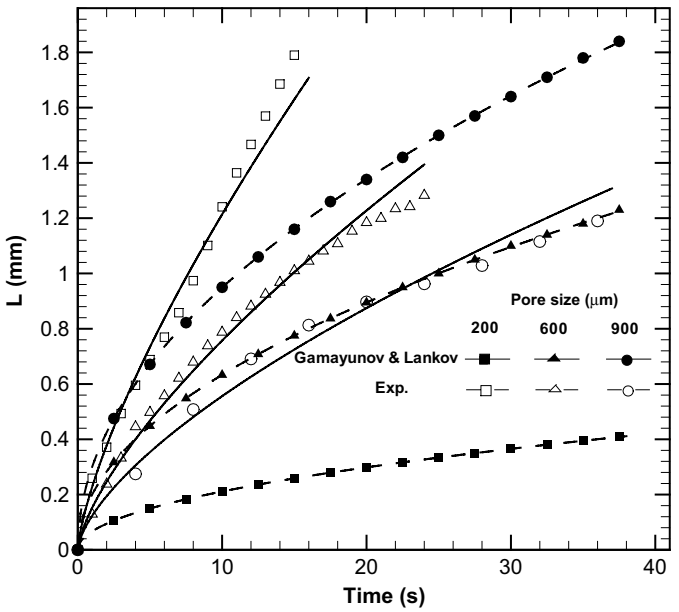

Fig. 15. Experiment (1): Gamayunov and Lankov (1985) present experimental comparison of the meniscus position (L) for n-pentane and various tube sizes.

and/or differential evaporation rate along the meniscus interface. The model of Gamayunov and Lankov (1985) reproduces well the trend of the curve found in the present experimental investigation (see Fig. 4) because the phenomena are diffusion controlled. However, Gamayunov and Lankov (1985) model fails in describing the effect of the tube size (see Fig. 15). It is believed that the discrepancy is mainly due to the observed enhancement because of the strong evaporation at the meniscus micro-region and the observed convection that helps in enhancing the heat–mass transfer at the meniscus interface.

6. Conclusion

Some fundamental aspects of the evaporation of volatile liquids from a meniscus formed in a confined space such as a capillary tube have been experimentally investigated. This is critical for a wide range of technological applications involving phase change in confined environment. The complex phenomena taking place in such applications can be modelled investigating a far simpler case such as the evaporation from a meniscus formed in a capillary tube. Four different liquids (ethanol, methanol, acetone and n-pentane) and three tube sizes (200, 600 and 900 μm) have been investigated in the present study. The non-uniform evaporation at the meniscus interface is responsible for a strong convection in the liquid phase driven by surface tension gradient. This paper describes the Marangoni convection in the meniscus liquid phase and how it enhances the heat and mass transfer from a pore. The Marangoni roll has been visualized using seeding particles and its characteristics (i.e., frequency, shape) have been measured. The evaporation rate was

also measured and correlated with the spinning frequency of convective patterns. Results show how both the average evaporation flux and the spinning frequency increases when reducing the tube size. Therefore, it was concluded that the heat and mass transfer from a pore is enhanced at smaller scales because of stronger evaporation and Marangoni convection.

Acknowledgements

The authors acknowledge the Engineering and Physical Sciences Research Council support through Grant/N02122. Prof. W. Easson (The University of Edinburgh) help to access PIV facility is recognized.

References

Berezhnoi, A.N., Semenov, A.V., 1997. Binary diffusion coefficients of liquid vapors in gases. Begell House Inc, New York.

Buffone, C., Sefiane, K., in press. IR measurements of interfacial temperature during phase change in a confined environment. Experimental Thermal and Fluid Science.

Chu, R.C., 1986. Heat transfer in electronic system. Proceeding of the Eighth International Conference on Heat Transfer, New York, USA, pp. 293–305.

Cook, R., Tung, C., Wayner, P., 1981. Use of scanning microphotometer to determine the evaporative heat transfer characteristics of the contact line region. J. Heat Transfer 103, 325–330.

Coulson, J.M., Richardson, J.J., 1999. Chemical Engineering, sixth ed., vol. 1. Elsevier, New York.

Davis, S.H., 1987. Thermocapillary instabilities. Annual Review of Fluid Mechanics 19, 403–435.

Deegan, R.D., Bakajin, O., Dupont, T.F., Huber, G., Nagel, S.R., Witten, T.A., 2000. Contact line deposit in an evaporating drop. Physical Review E 62, 756–765.

Dejaguin, B.V., 1965. Definition of the concept of disjoining pressure and its role in the statics and kinetics of thin layers of liquids. Colloid Journal USSR (Engl. Transl.) 17, 191–198.

Farshad, F., Rieke, H., Garber, J., 2001. New development in surface roughness measurements, characterization, and modeling fluid flow in pipe. J. Petroleum Science and Engineering 29, 139–150.

Gamayunov, N.I., Lankov, A.A., 1985. High-temperature evaporation of liquids from capillary tubes under the influence of a constant temperature gradient. Teplofizika Vysokikh Temperatur 23, 102–105.

Hallinan, K.P., Pratt, D.M., Brown, J.R., 1998. Thermocapillary effects on the stability of a heated meniscus. J. Heat Transfer 120, 220–226.

Khrustalev, D., Faghri, A., 1994. Heat Transfer during Evaporation and Condensation on Capillary-Grooved Structures of Heat Pipes ASME 287 (Advances in Enhanced Heat Transfer HTD), 47–59.

Khrustalev, D., Faghri, A., 1996. Fluid flow effects in evaporation from liquid–vapour meniscus. J. Heat Transfer 118, 725–730.

Kim, I.Y., 1994. An optical study of the heat transfer characteristics of an evaporating thin liquid film. Ph.D. Thesis, Rensselaer Polytechnic Institute, Troy, New York.

Lee, H.J., Fermín, D.J., Corn, R.M., Girault, H.H., 1999. Marangoni flow in micro-channels. Electrochemistry Communications 1, 190–193.

Li, Z.X., Du, D.X., Guo, Z.Y., 2002. Experimental study on flow characteristics of liquid in circular microtubes. Proceedings of the International Conference on Heat Transfer and Transport Phenomena in Microscale, Banff, Canada.

Meyer, R.E., 1984. Note on evaporation in capillaries. Journal of Applied Mathematics 32, 235–252.

Mirzamoghadam, A., Catton, I., 1988. A physical model of the evaporating meniscus. J. Heat Transfer 110, 201–207.

Molenkamp, T., 1998. Marangoni Convection, Mass Transfer and Microgravity. Ph.D. Thesis, University of Groningen, Germany.

Moosman, S., Homsy, S.M., 1980. Evaporating menisci of wetting fluids. Journal of Colloid and Interface Science 73, 212–223.

Park, K., Lee, K., 2003. Flow and heat transfer characteristics of the evaporating extended meniscus in a micro-capillary channel. Int. J. Heat and Mass Transfer 46, 4587–4594.

Potash, J.M., Wayner, J.P., 1972. Evaporation from a two-dimensional extended meniscus. Int. J. Heat and Mass Transfer 15, 1851–1863.

Pratt, D.M., 1996. The effects of thermocapillary stresses on the wetting characteristics, heat transfer effectiveness, and stability of an evaporating, capillary re-supplied, curved meniscus within a capillary tube. Ph.D. Thesis, University of Dayton, Ohio, USA.

Pratt, D.M., Hallinan, K.P., 1997. Thermocapillary effects on the wetting characteristics of a heated meniscus. J. Thermophysics and Heat Transfer 11, 519–525.

Riley, R.J., 1996. An investigation of the stability and control of a combined thermocapillary–buoyancy driven flow. Ph.D. Thesis, Georgia Institute of Technology, USA.

Sartre, V., Zaghdordi, M.C., Lallemand, M., 2000. Effect of interfacial phenomena on evaporative heat transfer in micro heat pipes. Int. J. Thermal Science 39, 498–504.

Schonberg, J.A., Dagupta, S., Wayner, P.C., 1995. An augmented Young–Laplace model of an evaporating meniscus in a microchannel with high heat flux. Experimental Thermal and Fluid Science 10, 163–170.

Shieh, C.-Y., 1985. Unsteady buoyancy thermocapillary induced convection in rectangular tank with phase change. Ph.D. Thesis, The University of Michigan, USA.

Swanson, L.W., Herdt, G.C., 1992. Model of evaporating meniscus in a capillary tube. J. Heat Transfer 114, 434–440.

Szymczyk, J., 1991. Marangoni and buoyant convection in a cylindrical cell under normal gravity. The Canadian J. Chemical Engineering 69, 1271–1276.

Wayner, J.P., Tung, C., 1985. Experimental study of evaporation in the contact line region of a thin film of hexane. J. Heat Transfer 107, 182–189.

Wei, Q., Ma, T., 2002a. Characteristics of two-phase flow and evaporating heat transfer in a capillary at constant heat fluxes. Proceedings of the International Conference on Heat Transfer and Transport Phenomena in Microscale, Banff, Canada.

Wei, Q., Ma, T., 2002b. Effects of the polarity of working fluid on vapor–liquid flow and heat transfer characteristics in a capillary. Proceedings of the International Conference on Heat Transfer and Transport Phenomena in Microscale, Banff, Canada.

Wei, Q., Ma, T., Miao, J., Wang, J., 2002. Effects of radius and heat transfer on the profile of evaporating thin liquid film and meniscus in capillary tubes. Int. J. Heat and Mass Transfer 45, 1879–1887.

Yaws, C.L., 1999. Chemical Properties Handbook. McGraw-Hill, New York.